

DYNAMICS OF SOCIAL SYSTEMS: COOPERATION AND FREE-RIDING

Yiping Ma (1, 2)

Mirta B. Gordon (1)

Jean-Pierre Nadal (3)

(1) Laboratoire Leibniz-IMAG, Grenoble
46, Ave. Félix Viallet, 38031 Grenoble Cedex 1, France
(mirta.gordon@imag.fr, web: <http://www-leibniz.imag.fr/Apprentissage>)

(2) Department of Physics, Hong Kong University of Science and Technology
Clear Water Bay, Kowloon, Hong Kong
(ph_myp@stu.ust.hk, http://ihome.ust.hk/~ph_myp/)

(3) Laboratoire de Physique Statistique, Ecole Normale Supérieure,
24 rue Lhomond, 75231 Paris cedex 05, France
(nadal@lps.ens.fr, <http://www.lps.ens.fr/~nadal>)

May 20, 2017

Abstract

We study the mean field dynamics of a model introduced by Phan et al [Wehia, 2005] of a polymorphic social community. The individuals may choose between three strategies: either not to join the community or, in the case of joining it, to cooperate or to behave as a free-rider. Individuals' preferences have an idiosyncratic component and a social component. Cooperators bear a fixed cost whereas free-riders support a cost proportional to the number of cooperators. We study the dynamics of this model analytically in the mean field approximation for both parallel and sequential updating. As we vary one of the parameters while keeping the other parameters fixed, the phase diagram experiences a rich class of bifurcations. Noticeably, a limit cycle is shown to exist in both parallel and sequential updating, under certain parameter settings. A comparison of the analytical predictions with computer simulations is also included.

Keywords: Social Networks Interactions, Dynamical Systems, Bifurcation.

1 Introduction

Recently [1, 2] a model was proposed to analyze social organizations whose members are expected to cooperate to a public good. Basic evidence on several kinds of communities, as well as data obtained in public goods experiments [3, 4], reveal a rough partition between individuals that cooperate to the public good and pure consumers (also called free-riders). This polymorphic configuration seems to be a stable form of organization.

The model corresponds to the following situation: individuals have to decide whether to join an organization or community. The members of the organization have to contribute to a task whose realization is beneficial for everybody. Cooperators bear a fixed cost for producing the public good for the community. The surplus of all the individuals, cooperators or not, increases proportionally to the number of cooperators. Individuals that do not cooperate are punished by cooperators through costless moral disapproval, which may be either a subjective moral burden, or a true sanction. This cost, proportional to the fraction of cooperators, is idiosyncratically weighted.

In the present paper, we consider the dynamical evolution of the model analytically, within a mean field approximation. Parallel and sequential updating are studied through the evolution of the corresponding map and flow respectively. They present different behaviors, depending on the models parameters.

The most striking result of our analysis is that for some range of parameter values and initial conditions, the trajectories of the flow reach the fixed points determined by Phan et al. [1] through quasi-cyclic paths that may last for very long times. The corresponding map exhibits a limit cycle. Thus, under such conditions, macroscopic fractions of individuals change their strategies successively. In experimental economics settings that correspond to parallel updating, true cycles might appear. In sequential updating, the transient oscillatory behavior of the system may be very long lasting, and should thus be observable in actual systems.

The paper is organized as follows: next section presents the details of the model and its equilibrium fixed points. Section 3 is devoted to the study of a mean field approximation of the dynamical equations. These describe the evolution of the fraction of cooperators and of free-riders. We consider both parallel and sequential updating, and study the corresponding map and flow. We show that the system may exhibit strong oscillations of the fraction of cooperators and of free-riders, and that limit cycles may exist for some range of the parameters. Numerical simulations presented in section 4 show that the predicted behaviours exist in finite size systems and might be observable in actual systems. The paper ends with a discussion and some conclusions.

2 The model

The basic economic model analyzed in this paper was introduced by Phan et al. [1]. It considers a system of N agents that must choose one among the following strategies:

$$\begin{aligned} S_i &= 1 & (\text{to join the community and cooperate}) \\ S_i &= 2 & (\text{to join the community and free-ride}) \\ S_i &= 3 & (\text{not to join the community}) \end{aligned}$$

Each individual i has a private idiosyncratic willingness to join the community, h_i . Its mean value over the population is h and we write: $h_i \equiv h + y_i$ where y_i is a quenched random variable with zero mean. Individuals that join the community have a social benefit proportional to the fraction of the population that join the community, weighted by a coefficient j , and an additional payoff proportional to the fraction of cooperators, weighted by a constant g . Then, depending on whether they cooperate or not, they bear different costs. A cooperator bears a fixed cost c . Free-riders do not bear this cost, but instead support a moral punishment proportional to the fraction of cooperators. This punishment is weighted by an idiosyncratic positive constant x_i . All the parameters of the model (h, j, g, c as well as the values of $\{y_i\}$ and $\{x_i\}$ for $1 \leq i \leq N$) are measured in units of the variance of the random variable y_i .

The fraction of cooperators is:

$$\eta_c \equiv \frac{1}{N} \sum_{i=1}^N \delta_{S_i,1},$$

where δ denotes the Kroenecker delta. That of free-riders is:

$$\eta_f \equiv \frac{1}{N} \sum_{i=1}^N \delta_{S_i,2},$$

so that the fraction of individuals that join the community is $\eta_a = \eta_c + \eta_f \leq 1$.

Each agent chooses the strategy that maximizes his surplus function,

$$V_i(S_i) = (A_i + B_i) \delta_{S_i,1} + A_i \delta_{S_i,2}. \quad (1)$$

A_i is the surplus of joining the community being free-rider, and B_i is the bonus of cooperating:

$$A_i = h + y_i + j(\eta_c + \eta_f) + (g - x_i)\eta_c, \quad (2a)$$

$$B_i = x_i\eta_c - c. \quad (2b)$$

From equation(1), the best response of agent i to the neighborhood's behavior can be rewritten as follows:

$$S_i = 1, \iff A_i + B_i > 0 \text{ and } B_i > 0; \quad (3a)$$

$$S_i = 2, \iff A_i > 0 \text{ and } B_i < 0; \quad (3b)$$

$$S_i = 3, \text{ otherwise} \quad (3c)$$

2.1 The Cluster Structure

In order to get some insight about the problem, it is useful to consider a plane whose axes are the quenched random variables x (abscissas) and y (ordinates), as in figure 1. Each individual i is represented by a point according to his values (x_i, y_i) . The lines represent the marginal individuals whose utilities are at the boundaries between different optimal strategies. These are:

$$y = y_m \equiv -h - j(\eta_c + \eta_f) - g\eta_c + c, \quad (4)$$

$$y = y_m - c + x\eta_c, \quad (5)$$

$$x = x_m \equiv \frac{c}{\eta_c}. \quad (6)$$

Then, according to (3), individuals in region I will choose to cooperate, in region II to free-ride and in region III not to join the community.

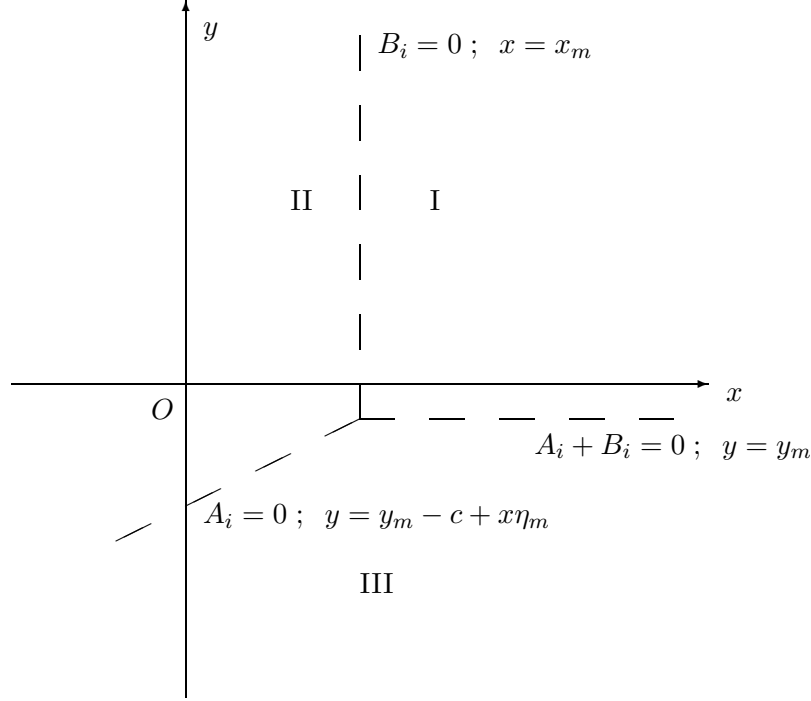


Figure 1: Boundaries between regions corresponding to the different individual choices, as a function of the values of the quenched random variables.

2.2 Fraction of cooperators and free-riders at equilibrium

The fixed points of the system for different distributions of the quenched random variables $\{x_i, y_i\}$ have been discussed in [1] and [2] in the mean field approximation $N \rightarrow \infty$. We summarize them here for completeness.

Introducing the complementary cumulative functions:

$$G_\chi(\zeta) \equiv 1 - F_\chi(\zeta) = \int_\zeta^\infty f_\chi(\xi) d\xi \quad (7)$$

where $\chi \in \{X, Y\}$, and $F_\chi(\zeta)$ is the cumulative distribution of f_χ , η_c and η_f have the following expressions in terms of the G functions and the marginal values (4):

$$\eta_c = G_X(x_m) G_Y(y_m), \quad (8a)$$

$$\eta_f = \int_0^{x_m} f_X(x) G_Y(y_m - c + x\eta_c) dx, . \quad (8b)$$

The solutions to equations (8) give the fraction of cooperators and free-riders at equilibrium as a function of the parameters of the problem, namely h, j, g, c, d (these parameters are measured in units of the variance of the distribution of y). Notice that

$\eta_c = 0$ is always solution of (8a), in which case all the members are free-riders, and the problem reduces to that of the simple social interactions model considered in [5, 6] and references therein. It is important to stress that, due to the non symmetric interaction x_i , there is no reason that the stationary states of the system be exclusively fixed points, as is the case for symmetric interactions¹.

In this paper we consider the most interesting of the cases analyzed in [1], with the x_i following a uniform distribution of finite width d :

$$f_X(x) = \frac{1}{d} \quad \text{for } 0 \leq x \leq d, \quad (9a)$$

$$f_X(x) = 0 \quad \text{otherwise.} \quad (9b)$$

and the y_i distributed according to the following probability density function:

$$f_Y(y) = \frac{1}{4 \cosh^2(y/2)}. \quad (10)$$

The cumulative function corresponding to (10) is the logistic distribution, and its complementary function is:

$$G_Y(z) = 1/[1 + \exp(z)]. \quad (11)$$

In this case, following Phan et al. [1], equations (8) may be written as follows:

$$\eta_c = (1 - \frac{\rho}{\eta_c}) G_Y(c - Z) \quad (12a)$$

$$\eta_f = \frac{\rho}{c\eta_c} \log[1 + (e^c - 1)G_Y(c - Z)], \quad (12b)$$

where $\rho \equiv c/d$ and $Z \equiv h + j(\eta_c + \eta_f) + g\eta_c$.

Calling G the value taken by $G_Y(c - Z)$, one has $\eta_c = (1 - \frac{\rho}{\eta_c}) G$, which gives η_c (if > 0) in terms of G :

$$\eta_c = \eta_c^\pm[G] \equiv \frac{1}{2}G \{1 \pm [1 - \frac{4\rho}{G}]^{1/2}\} \quad (13)$$

Later we'll see that both the + and the - branches may give stable equilibria, though the parameter range for which a stable equilibrium exists for the - branch is much narrower than for the + branch. The function $\eta_c^+[G]$ is very close to its asymptote, $G - \rho$, for all the values of G . From (13) one gets that if $\eta_c \neq 0$, then $\eta_c \geq 2\rho$. Equality can occur when $j = g = 0$.

Equation (12b) can also be parameterized in terms of G by defining

$$\eta \equiv \frac{j(\eta_c + \eta_f) + g\eta_c}{j + g}. \quad (14)$$

Introducing (13) and (12b) into (14) we obtain an equation for η :

$$\eta = \eta_1[G] \equiv \eta_c^\pm[G] + \frac{j}{j + g} \frac{1}{\eta_c^\pm[G]} \frac{1}{d} \log[1 + (e^c - 1)G] \quad (15)$$

¹In Ising systems, with binary microscopic states and symmetric interactions, the only attractors are fixed points for sequential dynamics, and either fixed points or cycles of order two for parallel dynamics.

Inverting (11) for $z = c - h - (j + g)\eta$, we obtain η in terms of G :

$$\eta = \eta_2[G] \equiv \frac{1}{j+g} \left\{ c - h - \log \frac{1-G}{G} \right\}. \quad (16)$$

The possible solutions η are then obtained by the intersects of the curves $\eta_1[G]$ and $\eta_2[G]$. Introducing the corresponding value of G into (13) allows to determine η_c , and then η_f is deduced by introducing the values of η_c and η into (14). An example of curves $\eta_1[G]$ and $\eta_2[G]$ ($G \in [0, 1]$) is shown on Figure (2), which presents up to 3 intersects (for $h - c = -3.3$), although one can check that at most 2 correspond to stable equilibria. Notice that this analysis allows to determine the fixed points of the system, but doesn't give any hint about the existence of cycles.

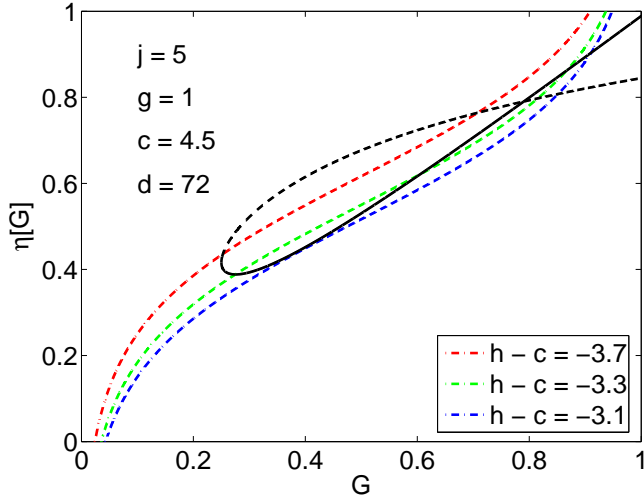


Figure 2: Solution by curve intersection - a case of interest.

3 Mean field dynamics

We are interested in the temporal evolution of the system within a repeated game setting, in which individuals have to choose their best strategies $S_i(t)$ based on the available information. We assume that each time an agent has to make a decision, he has the exact information of the global proportions of cooperators and free-riders at the preceding outcome, $\eta_c(t-1)$ and $\eta_f(t-1)$, and uses these quantities to estimate his utility (2). Such a dynamics is called Cournot best reply in economics literature. In simulations, starting from initial guesses $\eta_c(0)$ and $\eta_f(0)$, the updating is said to be in parallel if all the individuals in the population first determine their best strategies based on the preceding outcome, and make their decisions simultaneously afterwards. At the opposite, in random sequential updating, a single individual is selected at random and asked to make his decision at each time step. The latter dynamics simulates systems where the individuals make their decisions without any time coherence. In order to compare the time scales of both dynamics, it is usual to consider that N sequential

time steps are equivalent to one parallel update. Intermediate updating schemes may be implemented, but we only consider these two extreme cases in this paper.

Referring back to Figure 1, since the boundary lines depend on the values of $\eta_c(t)$ and $\eta_f(t)$, they will shift in the course of updating according to the perceived proportions of cooperators and free-riders. Individuals whose values of y_i and x_i lie close to the boundaries are susceptible to small changes of η_c and η_f : their strategies may change with time, and in turn induce changes in those of the others.

We are interested in the way the system reaches its stable states upon successive updates, that is, the path followed by a point representative of the system's state in the plane (η_c, η_f) . Such paths should either end up in one of the stable fixed points determined by the previous analysis, or get trapped in other types of attractors if they exist. In the following we consider separately the two updating schemes, since the corresponding dynamic equations are different.

3.1 Parallel dynamics: two-dimensional map

In parallel dynamics, one assumes that the agents are updated simultaneously starting from an arbitrary initial configuration, i.e. the perceived η_c and η_f used by all the agents to estimate their utilities are the same. The boundary lines between the three regions of figure 1, which depend on $\eta_c(t)$ and $\eta_f(t)$, partition the population at time t according to their estimated utilities: all the individuals whose idiosyncratic parameters lie in region I will choose to cooperate, those in region II to free-ride and those in region III not to join. In this way, using equations (8), the dynamics can be formulated as the following two-dimensional deterministic map in the simplex $\mathbf{S} := \{(\eta_c, \eta_f) : \eta_c \geq 0, \eta_f \geq 0, \eta_c + \eta_f \leq 1\}$:

$$\Omega : (\eta'_c, \eta'_f) = (p(\eta_c, \eta_f), q(\eta_c, \eta_f)) \quad (17a)$$

$$\equiv \left(\int_{x_m}^{\infty} f_X(x) dx \int_{y_m}^{\infty} f_Y(y) dy, \int_{-\infty}^{x_m} \int_{y_m - c + x\eta_c}^{\infty} f_X(x) f_Y(y) dy dx \right). \quad (17b)$$

In the case considered in this paper, the density functions are (9) and (10). Since f_X has a bounded support, the first equation vanishes if $0 < \eta_c(t) < \rho$. Thus, if the initial value of η_c is such that $\eta_c(0) < \rho$, then $\eta_c(1) = 0$ and a state with no cooperator is reached after a single parallel update. Afterwards, on the axis $\eta_c = 0$, η_f evolves according to

$$\eta_f(t+1) = \int_{-h-j\eta_f(t)}^{\infty} f_Y(y) dy. \quad (18)$$

The equilibrium value of η_f is obtained replacing $\eta_f(t)$ by η_f in the above equation. It has been shown [7] that there is a critical value of j , j_B , such that for $j < j_B$, there is a single equilibrium. In that case all the points $\eta_c(0) < \rho$ will eventually be mapped to it. If $j > j_B$ equation (18) with $\eta_f(t) = \eta_f$ has three solutions. One of them, η_{fu} is an unstable fixed point separating the basin of attraction of the two others, that are stable. To summarize, when $\eta_c(0) < \rho$, after a first time step the system is mapped to the axis $\eta_c = 0$ and then evolves, following (18), either to one fixed point (if $j < j_B$) or to one of two fixed points (if $j > j_B$) depending on whether $\eta_f(0) > \eta_{fu}$ or $\eta_f(0) < \eta_{fu}$. In the case of the logistic distribution considered here, $j_B = 4$.

When $\eta_c(0) > \rho$, the dynamics is most fruitfully studied numerically. In two-dimensional maps or flows, a fixed point is called a sink if all the points in its neighborhood converge to it, a source if these points diverge from it and a saddle if in one direction the map or flow converges, while in the other directions it diverges. Together these three types are called hyperbolic, which is the only kind of equilibria possibly encountered in a structurally stable system, i.e. a system stable with respect to small variations of the parameters (in our case h , j , g , c and d). For our two-dimensional map, the nature of an equilibrium point (η_{c0}, η_{f0}) is determined by the following Jacobian matrix

$$\mathbf{J}_m = \begin{bmatrix} \partial p(\eta_{c0}, \eta_{f0}) / \partial \eta_c & \partial p(\eta_{c0}, \eta_{f0}) / \partial \eta_f \\ \partial q(\eta_{c0}, \eta_{f0}) / \partial \eta_c & \partial q(\eta_{c0}, \eta_{f0}) / \partial \eta_f \end{bmatrix}.$$

Denoting the two eigenvalues of \mathbf{J}_m as a_1 and a_2 , then the fixed point is a sink if $|a_1| < 1$ and $|a_2| < 1$, a source if $|a_1| > 1$ and $|a_2| > 1$ and a saddle if $(|a_1| - 1)(|a_2| - 1) < 0$ ([8]§1.4). There are two types of curves emanating from each saddle point x_0 , namely the stable manifold, defined as

$$W_s(x_0) = \{x \in \mathbb{R}^2 | \Omega^n(x) \rightarrow x_0 \text{ as } n \rightarrow \infty\} \quad (19)$$

and the unstable manifold, defined as

$$W_u(x_0) = \{x \in \mathbb{R}^2 | \Omega^{-n}(x) \rightarrow x_0 \text{ as } n \rightarrow \infty\} \quad (20)$$

Ω^{-1} denoting a backward iterate of the map. The boundaries of the basins of attraction are usually formed by stable manifolds. Moreover, if a transversal intersection between the stable and unstable manifolds of the same saddle point exists, the map will exhibit chaotic behavior.

In view of their crucial importance, we have numerically computed the stable and unstable manifolds for each saddle point, with the same set of j , g , c and d as in Figure 2, while changing $h - c$ from -4 to -3 in steps of 0.02 . The algorithms used to compute the stable and unstable manifolds can be found in [9] and Chapter 10 of [10], respectively. The results classified according to the qualitative dynamical features are shown in Figures (3-8). Hereafter we provide the increasing values of $h - c$, denoted by λ_i , at which the successive bifurcations appear, together with the qualitative descriptions of their nature.

- $\lambda_1 = -4.0971$. For $h - c < \lambda_1$ there exists no intersection between $\eta_1(G)$ and $\eta_2(G)$ and all the points in \mathbf{S} are eventually mapped to the trivial fixed point, which is always a solution of the equations. At $h - c = \lambda_1$, $\eta_2(G)$ begins to intersect $\eta_1^-(G)$ at two points, one of which is a saddle (H_-) and the other is a source (X_-) (Figure 3). The process of simultaneous creation or elimination of a pair of equilibrium points is called a saddle-node bifurcation. Note that this bifurcation does not alter the overall behavior of the system, since no new attractor is created. Thus, only the fixed points $\eta_c = 0$, $\eta_f > 0$ exist, and since $j > j_B$, the system may flow to either of the two fixed points for η_f depending on the initial conditions.

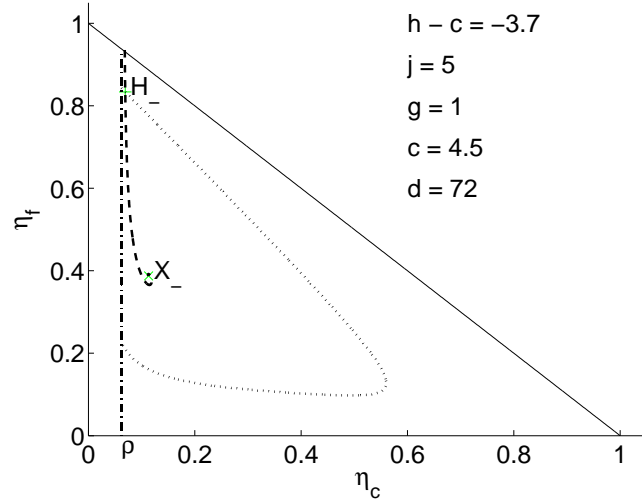


Figure 3: Map. The stable and unstable manifolds for $h - c = -3.7$. Throughout this article, stable manifolds are represented by dashed lines and unstable manifolds by dotted lines. It's well understood from their definitions that an arbitrary initial point on the stable manifold will be mapped towards the saddle from which it emanates, while one on the unstable manifold will be mapped away from it. Sinks, sources and saddles are represented by O, X, and H respectively, and the subscripts describe the branch $(\eta_1^+(G)/\eta_1^-(G))$ on which the equilibrium is found.

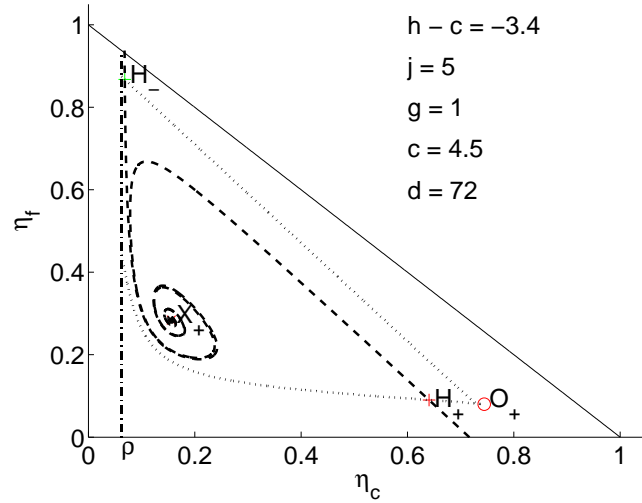


Figure 4: Map. H_+ and O_+ have been created from a saddle node bifurcation on $\eta_1^+(G)$.

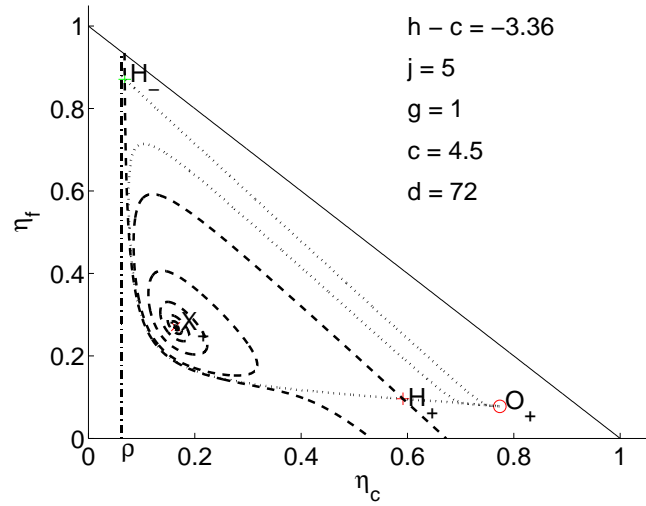


Figure 5: Map. A separatrix bifurcation between the stable manifold of H_- and the unstable manifold of H_+ has introduced a first order transition in the basin of attraction.

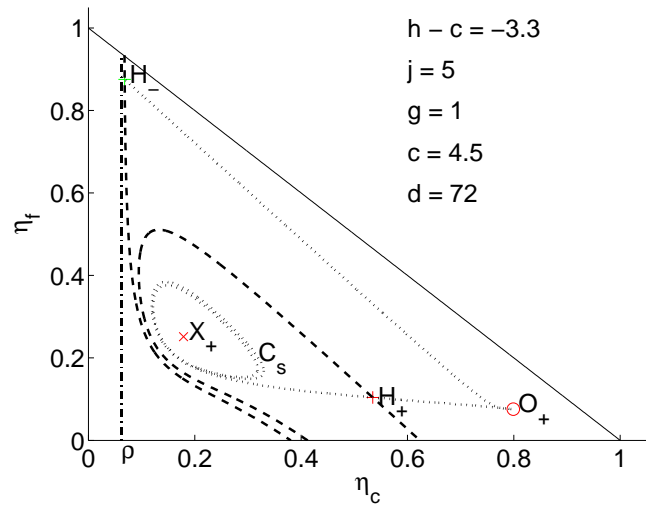


Figure 6: Map. A separatrix bifurcation between the stable and unstable manifolds of H_+ has introduced a stable cycle C_s with its own basin of attraction.

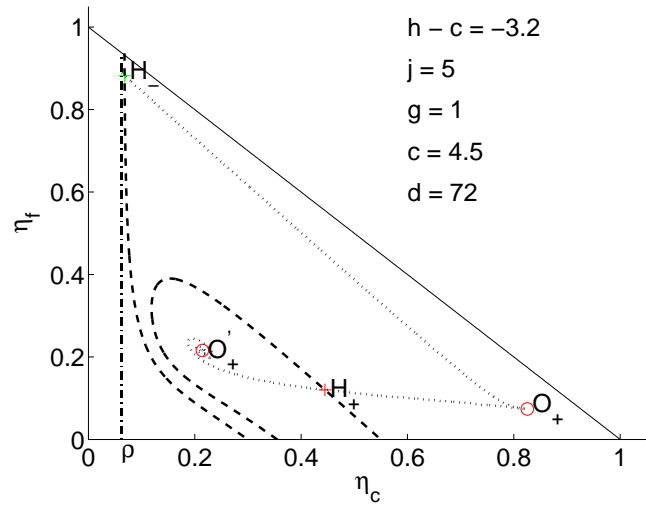


Figure 7: Map. The stable limit cycle C_s has merged with the source X_+ through a Hopf bifurcation to become a sink O'_+ .

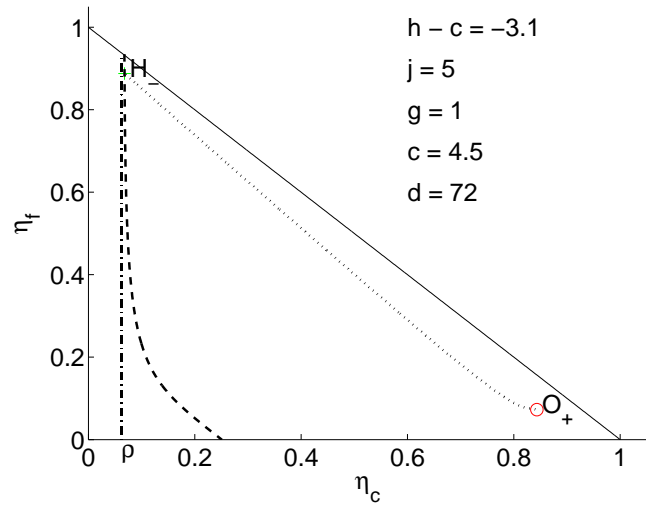


Figure 8: Map. A final saddle node bifurcation has annihilated O'_+ and H_+ .

- $\lambda_2 = -3.4201$. Another saddle-node bifurcation happens on $\eta_1^+(G)$ at $h - c = \lambda_2$, with a saddle (H_+) and a sink (O_+) created simultaneously (Figure 4). Now the stable manifolds of H_+ and H_- possess a common end emanating from X_+ , and together they divide \mathbf{S} into two regions. Points outside the region bounded by the stable manifolds should converge to the trivial fixed point $\eta_c = 0, \eta_f > 0$ as before, and those inside to O_+ .
- $\lambda_3 = -3.3617$. For $\lambda_2 < h - c < \lambda_3$, the unstable manifold of H_+ approaches the stable manifold of H_- until they coincide at $h - c = \lambda_3$ (the common manifold is called a separatrix between H_+ and H_-). Beyond this value, the unstable manifold of H_+ folds back and converges to O_+ while the stable manifold of H_- hits the simplex boundary $\eta_f = 0$ (Figure 5). Now the basin boundary is determined solely by the stable manifold of H_- , causing the basin of attraction of O_+ to experience a sudden expansion.
- $\lambda_4 = -3.3504$. For $\lambda_3 < h - c < \lambda_4$, the stable and unstable manifolds of H_+ approach each other until they coincide at $h - c = \lambda_4$. Beyond this value, the former ends up at the boundary $\eta_f = 0$ of \mathbf{S} and the latter folds back into a stable limit cycle C_s around X_+ (Figure 6). At this transition C_s is introduced into the system as a new attractor with its own basin of attraction delimited by the stable manifold of H_+ .
- $\lambda_5 = -3.2726$. For $\lambda_4 < h - c < \lambda_5$, C_s shrinks and eventually merges with X_+ at $h - c = \lambda_5$ to produce a sink O'_+ (Figure 7). The process of transition between a sink and a source with the simultaneous appearance or disappearance of a limit cycle is called a Hopf bifurcation.
- $\lambda_6 = -3.1146$. For $\lambda_5 < h - c < \lambda_6$, O'_+ and H_+ approach each other until they are annihilated at $h - c = \lambda_6$. We are left with H_- and O_+ , the stable manifold of H_- serving as the basin boundary (Figure 8). This topology persists for arbitrarily larger values of $h - c$.

Summarizing the analysis above, we can identify three types of transition:

1. saddle-node bifurcation;
2. Hopf bifurcation;
3. separatrix bifurcation between two saddle points, or one saddle point with itself.

Type 1 can be directly determined from the number of intersections between $\eta_1(G)$ and $\eta_2(G)$ (cf. figure 2), or from the fact that \mathbf{J}_m has an eigenvalue $+1$. Due to the lack of symmetry in our system, transcritical and pitchfork bifurcations never occur ([8] §3.4). In case that \mathbf{J}_m has an eigenvalue -1 , one can have a period-doubling bifurcation ([8] §3.5). This never happens in our map, since one can easily verify that

$$\mathbf{J}_m(1,1) > 0, \quad \mathbf{J}_m(2,2) > 0, \quad \Delta(\mathbf{J}_m) > 0, \quad (21)$$

which excludes the possibility that \mathbf{J}_m has a negative eigenvalue.

Types 2 and 3 cannot be observed from the intersections between $\eta_1(G)$ and $\eta_2(G)$ and must be determined numerically. Type 2 remains a local bifurcation with \mathbf{J}_m having a pair of conjugate complex eigenvalues with unit modulus. In contrast, Type 3 is a global bifurcation with the area of the basin of attraction experiencing a sudden jump or, in physicist's terms, a first-order transition. Numerically we have found no evidence for homoclinic intersection leading to chaos, but the question as to whether chaos exists in our two-dimensional map remains open.

3.2 Sequential dynamics: two-dimensional flow

In sequential dynamics, one updates one agent chosen at random in each time step. It is usual to consider N (the number of agents in the system) successive random sequential updates (called one Monte-Carlo step) as being comparable to one step of parallel updating.

In each individual update, the expected displacement of the pair (η_c, η_f) is

$$(\overline{\Delta\eta_c}, \overline{\Delta\eta_f}) = \frac{1}{N}(p(\eta_c, \eta_f) - \eta_c, q(\eta_c, \eta_f) - \eta_f), \quad (22)$$

where p and q are defined in (17). Taking the continuous limit $N \rightarrow \infty$, we have the following set of differential equations

$$d\eta_c/dt = p(\eta_c, \eta_f) - \eta_c, \quad (23a)$$

$$d\eta_f/dt = q(\eta_c, \eta_f) - \eta_f, \quad (23b)$$

with the time unit being one Monte-Carlo step. Now the community evolves as an autonomous system with planar phase space, or a two-dimensional flow in \mathbf{S} .

The three generic types of equilibria, namely source, sink and saddle exist in a structurally stable two-dimensional flow as well. However, the nature of an equilibrium point (η_{c0}, η_{f0}) is now determined by the Jacobian matrix of the flow

$$\mathbf{J}_f = \begin{bmatrix} \partial p(\eta_{c0}, \eta_{f0})/\partial\eta_c - 1 & \partial p(\eta_{c0}, \eta_{f0})/\partial\eta_f \\ \partial q(\eta_{c0}, \eta_{f0})/\partial\eta_c & \partial q(\eta_{c0}, \eta_{f0})/\partial\eta_f - 1 \end{bmatrix}.$$

Denoting the eigenvalues of \mathbf{J}_f as a_1 and a_2 , then the point is a sink if $a_1 < 0$ and $a_2 < 0$, a source if $a_1 > 0$ and $a_2 > 0$ and a saddle if $a_1 a_2 < 0$ ([8] §1.2~1.3). Note that the condition for an equilibrium to be a saddle gives the same inequality as in the parallel case. Therefore, the set of saddle points in sequential updating coincides with that in parallel updating. However, the set of sinks or sources are not necessarily the same in both cases, since the governing inequalities are quite different. The definitions of the stable and unstable manifolds are analog to those in the two-dimensional map with the discrete time step replaced by the continuous time variable t . However, we note that the two-dimensional flow system, according to the Poincaré-Bendixson Theorem ([8] Theorem 1.8.1), will never go into chaos.

We have computed the stable and unstable manifolds as for the map. The results shown in Figures (9-13). Hereafter we provide the bifurcation values of $h - c$, denoted by μ_i , together with the qualitative descriptions of the nature of the bifurcation:

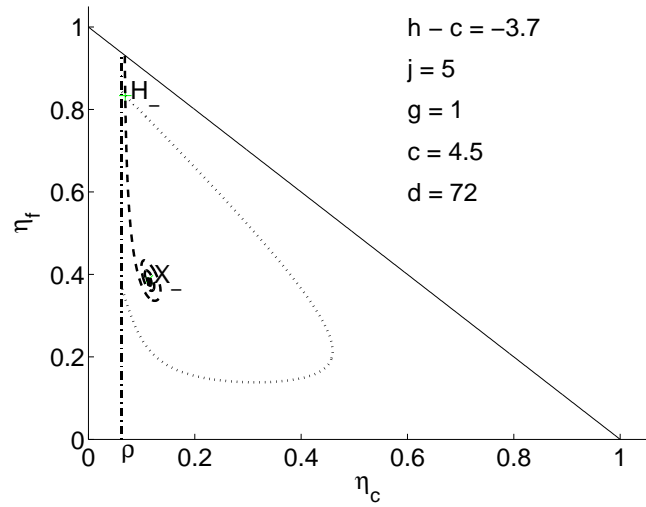


Figure 9: Flow. The stable and unstable manifolds for the flow. Compare with Figure 3.

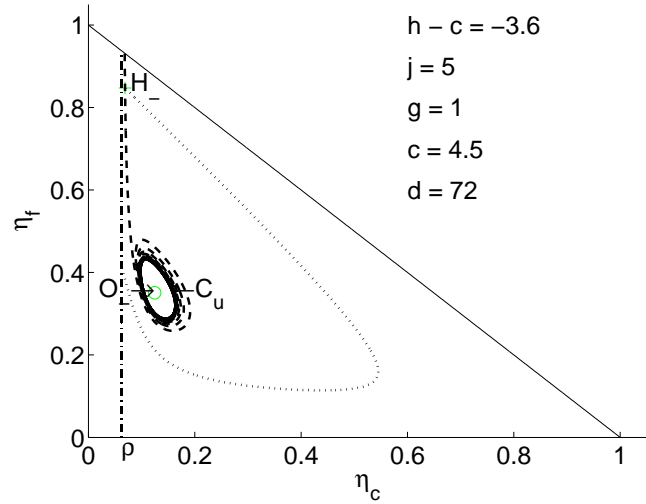


Figure 10: Flow. A sink O_- together with an unstable limit cycle C_u has emerged from the source X_- through a Hopf bifurcation.

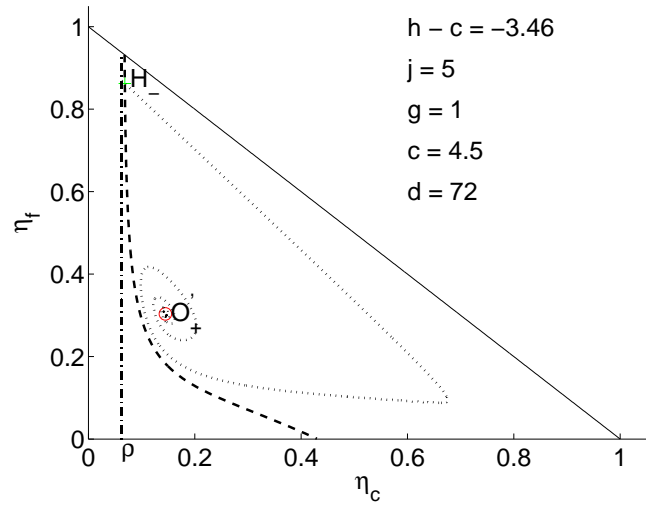


Figure 11: Flow. A separatrix bifurcation has eliminated C_u and expanded the basin of attraction of the sink.

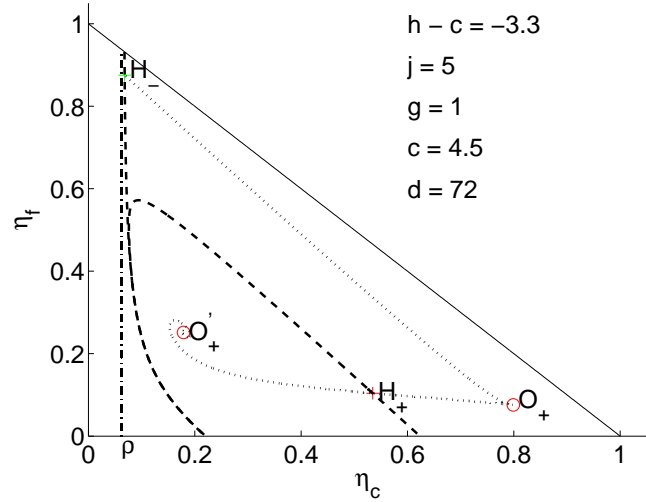


Figure 12: Flow. H_+ and O_+ have been created from a saddle node bifurcation on $\eta_1^+(G)$. Compare with Figure 6.

- $\mu_1 = \lambda_1 = -4.0971$. As in the parallel case, a saddle node bifurcation occurs at $h - c = \mu_1$ and produces a saddle H_- and a source X_- (Figure 9).
- $\mu_2 = -3.6172$. A Hopf bifurcation occurs at $h - c = \mu_2$ and produces an unstable limit cycle C_u together with a sink O_- from the source X_- (Figure 10). The basin of attraction of O_- is the area surrounded by C_u . Note that we've been able to choose $h - c$ such that the sink remains in the negative branch, which implies that variation of η with respect to $h - c$ does not always qualify to determine the stability of the fixed point.
- $\mu_3 = -3.4980$. A separatrix bifurcation of the stable and unstable manifolds of H_- eliminates C_u (Figure 11).
- $\mu_4 = \lambda_2 = -3.4201$. A saddle node bifurcation occurs at $h - c = \mu_4$ and produces a sink O_+ and a saddle H^+ (Figure 12).
- $\mu_5 = \lambda_6 = -3.1146$. A saddle node bifurcation occurs at $h - c = \mu_5$ and annihilates the saddle H_+ and the source O'_+ . The topology persists for larger $h - c$ (Figure 13).

Thus, we have the same types of bifurcation as in the parallel case, and Peixoto's Theorem ([8] Theorem 1.9.1) indicates that these are the only types of bifurcation expected in a two-dimensional flow system. However, let's note that the overall topology of the dynamics depends strongly on their order of occurrence. For example, if the separatrix bifurcation happens before the Hopf bifurcation, a stable limit cycle can be created just like in the parallel case (Figure 14).

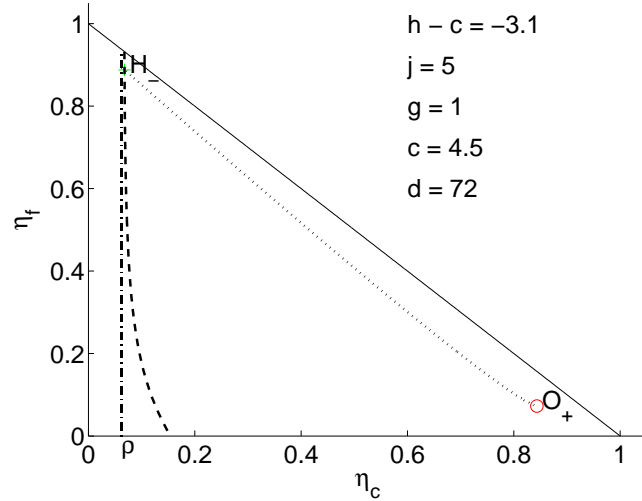


Figure 13: Flow. A final saddle node bifurcation has annihilated O'_+ and H_+ . Compare with Figure 8.

4 Comparison with Computer Simulations

We simulated systems of $N = 1000$ agents, corresponding to the parameter values of figures 15 to 20, with parallel dynamics. Starting from different initial conditions, we determined the trajectories in the phase space (η_c, η_f) . The results, presented on figures 15 to 20 show an excellent agreement with the analytical results. The complexity of the map diagram is reflected on the winding trajectories. One of the most striking results of the simulations is that the fraction of cooperators and free-riders oscillate in time, even in systems for which do not expect to have cycles.

5 Conclusion

In this paper we have studied the time evolution of a social system with cooperators and free-riders. We analyzed the two-dimensional dynamical system and obtained different phase diagrams corresponding to various parameter settings. The fact that a rich class of bifurcations can occur within the narrow tubular region enclosed by the curves $h - c = -3.7$ and $h - c = -3.1$ in Figure (2) is in itself truly remarkable. Physically this phenomenon has its root in the strong asymmetry inherent in the interaction between agents, due to the idiosyncratic weights that the free-riders give to the social disapproval. Moreover, in the context of parallel and sequential updating, we have sometimes distinctly different phase diagram for the same parameter setting. A natural question to ask is what happens in the intermediate case, i.e. some agents' decisions are taken simultaneously while others' decisions are taken independently of each other. Numerical simulations show that the analytical results obtained in the thermodynamic limit are valid for systems of $N = 1000$ individuals. The dynamical behaviour of the simulated systems show winding trajectories in very large regions of the phase diagram. Oscillations of the fraction of cooperators and free-riders are thus expected in such systems. We are currently performing simulations with sequential

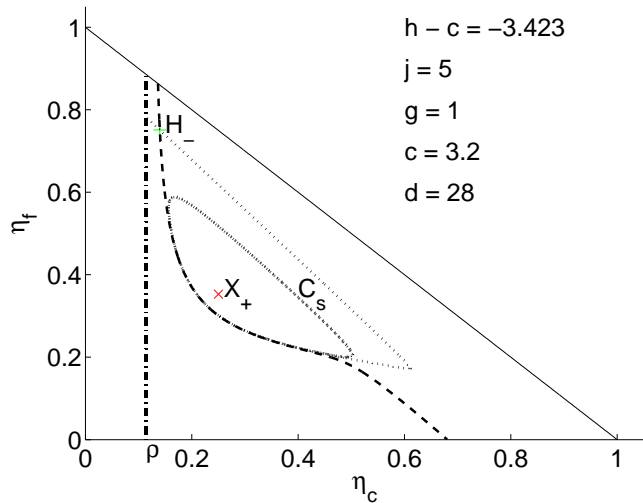


Figure 14: Flow. A stable limit cycle in the two-dimensional flow.

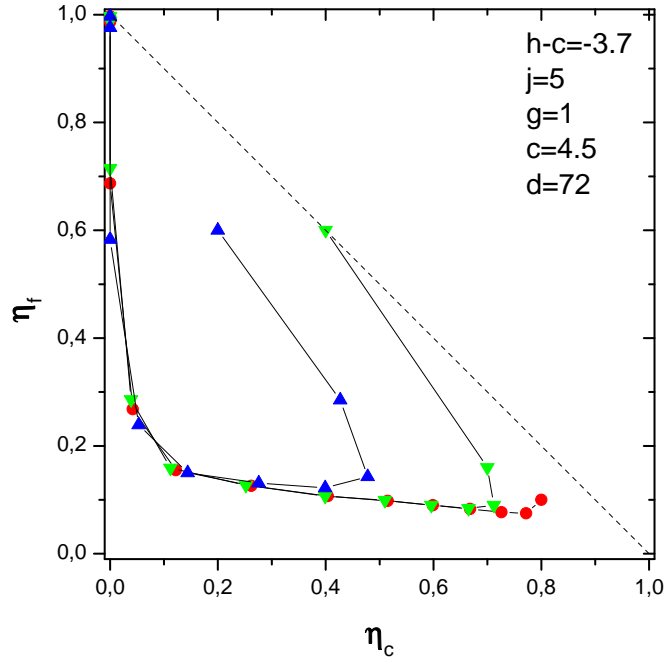


Figure 15: Examples of trajectories of a simulated system, starting from different initial conditions, corresponding to the map of figure 3.

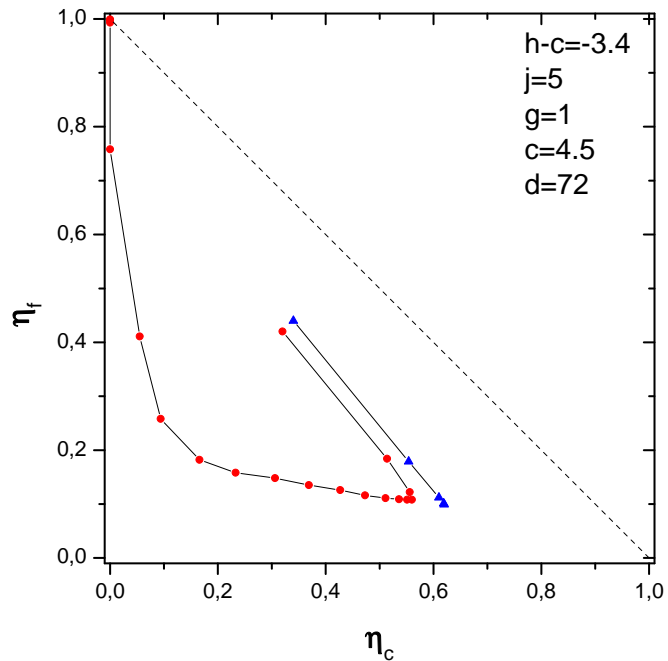


Figure 16: Examples of trajectories of a simulated system, starting from different initial conditions, corresponding to the map of figure 4.

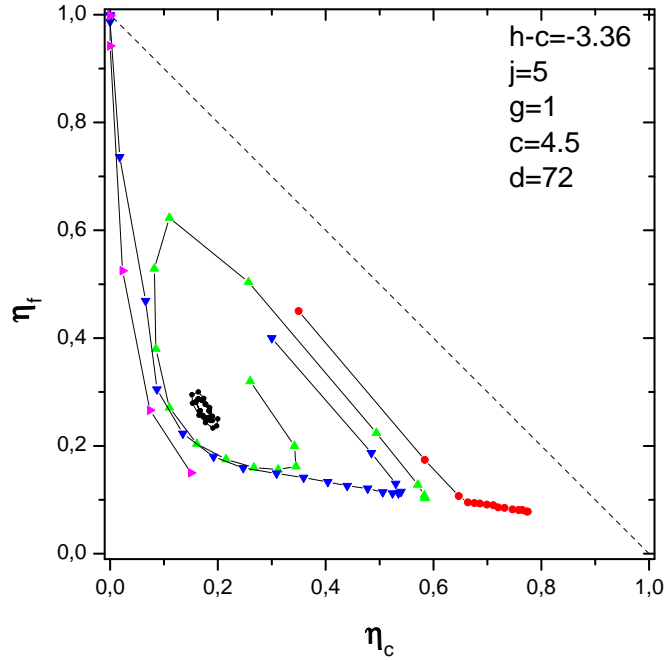


Figure 17: Examples of trajectories of a simulated system, starting from different initial conditions, corresponding to the map of figure 5.

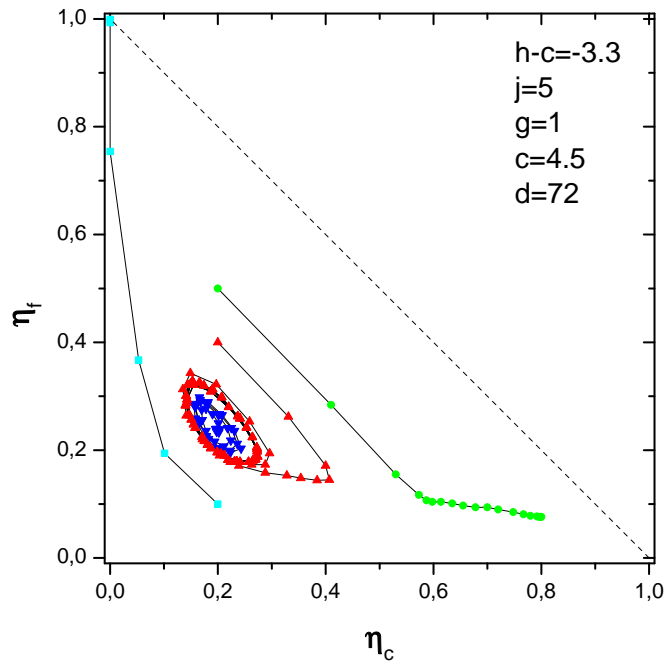


Figure 18: Examples of trajectories of a simulated system, starting from different initial conditions, corresponding to the map of figure 6.

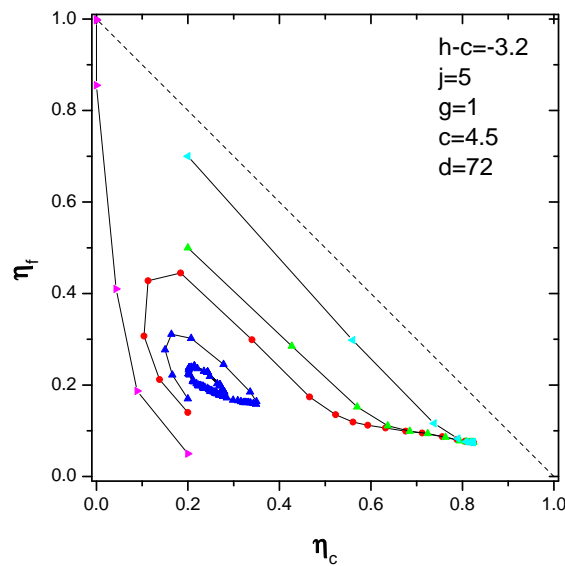


Figure 19: Examples of trajectories of a simulated system, starting from different initial conditions, corresponding to the map of figure 7.

dynamics. Already obtained results also exhibit the above mentionned oscillatory behaviour. Future work can also focus on the dynamics in the case of non-global neighborhood, which probably requires more sophisticated techniques from the theory of dynamical systems.

References

- [1] Denis Phan, Roger Waldeck, Mirta B. Gordon and Jean-Pierre Nadal (2005), *Adoption and cooperation in communities: mixed equilibrium in polymorphic populations*; Annual Workshop on Economics with Heterogeneous Interacting Agents - WEHIA 2005, June 13-15, University of Essex, UK
- [2] M. B. Gordon, D. Phan, R. Waldeck and J.-P. Nadal (2005), *Cooperation and free-riding with moral cost*; Proceedings of International Conference on Cognitive Economics (ICCE), Sofia-Bulgaria
- [3] E. Fehr and S. Gaechter (2002), *Altruistic Punishment in Humans*; Nature 415 137-140
- [4] S. Gaechter and E. Fehr (1999), *Collective Action as a Social Exchange*; Journal of Economic Behavior and Organization 39 341-369
- [5] S. N. Durlauf (2001), *A framework for the study of individual behaviour and social interactions*; Working paper

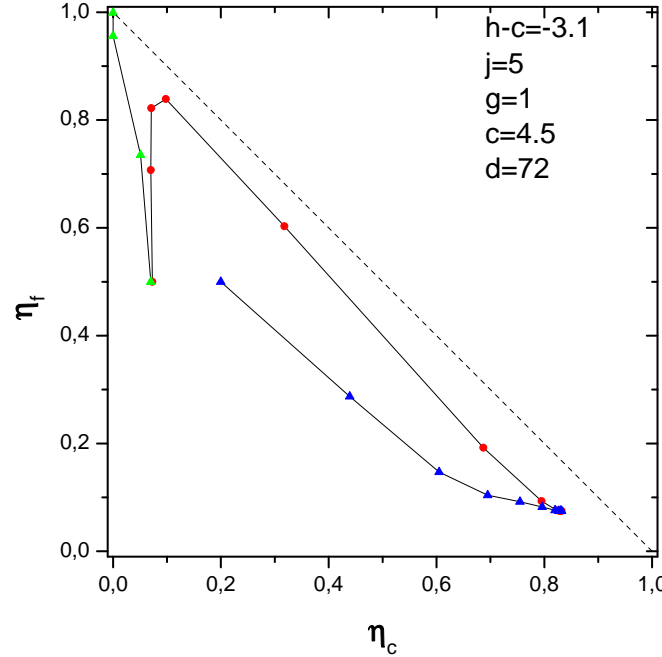


Figure 20: Examples of trajectories of a simulated system, starting from different initial conditions, corresponding to the map of figure 8.

- [6] M. B. Gordon, J.-P. Nadal, D. Phan and J. Vannimeuns (2005), *Seller's dilemma due to social interactions between customers*; *Physica A* 356, Issues 2-4 628-640
- [7] J-P. Nadal, D. Phan, M. B. Gordon and J. Vannimenus (2005), *Multiple equilibria in a monopoly market with heterogeneous agents and externalities*; *Quantitative Finance*, to be published
- [8] J. Guckenheimer and P. Holmes (1990), *Nonlinear oscillations, dynamical systems, and bifurcations of vector fields*; Springer-Verlag
- [9] J. P. England, B. Krauskopf and H. M. Osinga (2004), *Computing One-Dimensional Stable Manifolds and Stable Sets of Planar Maps without the Inverse*; *SIAM Journal on Applied Dynamical Systems*
- [10] K. Alligood, T. Sauer and J.A. Yorke (1997), *Chaos: An Introduction to Dynamical Systems*; Springer-Verlag